PROCEEDINGS of the
23rd International Congress on Acoustics
9 to 13 September 2019 in Aachen, Germany

Calculation of wave propagation characteristics in pre-deformed periodic lattice frame structures via Spectral Element Method

Marius MELLMANN[1]*; Chuanzeng ZHANG[1]

[1]Chair of Structural Mechanics, University of Siegen, Germany

Abstract

In recent years, the design, optimization and application of periodic materials and structures, such as phononic and photonic crystals, are becoming popular in many engineering fields. For instance, the phononic crystals can manipulate the elastic and acoustic wave propagation characteristics. Consequently, it is feasible to create the so-called band-gaps, which are certain frequency ranges, in which the propagation of elastic or acoustic waves is prohibited (1, 2). Accordingly, such structures have many promising applications in sound and vibration insulation as well as wave filters. In this paper, the dispersion curves of pre-deformed periodic lattice frame structures are calculated using the Spectral Element Method (SEM), which is based on the exact solution of the elastic wave equations. Numerical examples will be presented and compared with FEM calculations.

Keywords: Periodic lattice structures, Phononic crystals, Spectral Element Method (SEM)

1 INTRODUCTION

For periodic lattice frame structures, it is possible to manipulate the vibration and elastic wave propagation properties by altering the stiffness and density of the structural members or by adding local resonators. In addition to the change of the stiffness and mass of the system, it is also possible to control the vibration and wave propagation properties by means of a specific pre-deformation of the structural elements, such as shown in Figure 1 (3, 4). The vibration and wave propagation characteristics of such structures can be obtained by considering a representative unit-cell with imposed Bloch-Floquet boundary conditions and calculating the corresponding dispersion curves. This calculation can be carried out by different numerical methods such as the FEM, FDM, Plane Wave Expansion (PWE) Method and Layered Multiple Scattering (LMS) Method (5). In this paper the dispersion curves of pre-deformed periodic lattice frame structures are calculated using the Spectral Element Method (SEM), which is based on the exact solution of the elastic wave equations. This results in the advantage, that it is sufficient to represent each beam with just one spectral element and the eigenvalue calculation still yields the exact eigenfrequencies.

Figure 1. Pre-deformation of a periodic lattice structure.

2 SPECTRAL ELEMENT METHOD

The Spectral Element Method used in this paper is based on the approach by Doyle (6) which uses the exact solution of the elastic wave equations to derive spectral element matrices. This method is not to be mistaken for the Spectral Element Method proposed by Patera (7) which is based on the FEM with high order shape functions. The approach by Doyle begins by transforming the governing partial differential equations of motion from the time domain into the frequency domain via Fourier-Transformation. Consequently, the time variable is replaced by the frequency variable and the time-domain partial differential equations are transformed

*Corresponding author: mellmann@bau.uni-siegen.de

into frequency-domain ordinary differential equations. Subsequently, these equations are solved exactly and by using the exact wave solutions frequency-dependent dynamic shape functions are derived (8). By means of the dynamic shape functions the exact dynamic stiffness matrix, called the spectral element matrix, is finally formulated similarly to the procedure commonly used in FEM (8).

In the following sections the derivation of the spectral element matrices for the rod and the Euler-Bernoulli beam are presented. The formulation is based on the force-displacement relation method. For other methods of spectral element formulation, like the variational method or the state-vector equation method, we refer to (8).

2.1 Derivation of the spectral element matrix for a rod

The partial differential equation of motion for free longitudinal vibration of a rod is given by

$$EAu'' - \rho A\ddot{u} = 0, \tag{1}$$

where $u(x,t)$ is the longitudinal displacement, E is the Young's modulus, A is the cross-sectional area and ρ is the mass density. The solution of Eq. 1 is assumed as

$$u(x,t) = \frac{1}{N}\sum_{n=0}^{N-1} U_n(x,\omega_n)\mathrm{e}^{i\omega_n t}. \tag{2}$$

Substituting the approach of Eq. 2 into Eq. 1 yields the eigenvalue problem

$$EAU'' + \omega^2 \rho AU = 0 \tag{3}$$

for each discrete frequency ω_n. The general solution of Eq. 3 is assumed to be

$$U(x) = a\mathrm{e}^{-ik(\omega)x}. \tag{4}$$

Substituting Eq. 4 in Eq. 3 yields the dispersion relation

$$k^2 - k_L^2 = 0 \tag{5}$$

with the two real roots

$$k_1 = -k_2 = k_L, \tag{6}$$

where k_L is the wave number of the longitudinal wave mode and is given by

$$k_L = \omega\sqrt{\frac{\rho A}{EA}}. \tag{7}$$

Finally, by inserting the roots in Eq. 4 the general solution for a finite rod element of length L is given by

$$U(x) = a_1\mathrm{e}^{-ik_L x} + a_2\mathrm{e}^{ik_L x} = \boldsymbol{e}(x,\omega)\boldsymbol{a} \tag{8}$$

with

$$\boldsymbol{e}(x,\omega) = \left[\mathrm{e}^{-ik_L x}\ \mathrm{e}^{ik_L x}\right], \quad \boldsymbol{a} = [a_1\ a_2]^T. \tag{9}$$

The values of $\boldsymbol{a}$ depend on the spectral nodal displacements of the finite rod element, pictured in Figure 2, which can be related to the displacement field via

$$\boldsymbol{d} = [U_1\ U_2]^T = [U(0)\ U(L)]^T. \tag{10}$$

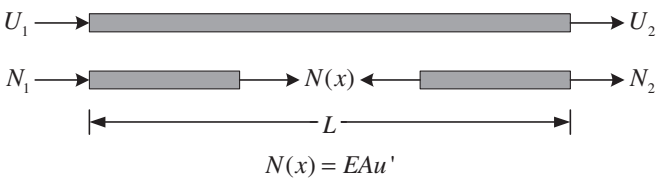

Figure 2. Sign convention for the rod element.

Evaluating Eq. 8 at these nodes yields

$$\boldsymbol{d} = [\boldsymbol{e}(0,\omega)\ \ \boldsymbol{e}(L,\omega)]^T \boldsymbol{a} = \boldsymbol{H}_R(\omega)\boldsymbol{a} \tag{11}$$

where

$$\boldsymbol{H}_R(\omega) = \begin{bmatrix} 1 & 1 \\ \mathrm{e}^{+ik_L L} & \mathrm{e}^{-ik_L L} \end{bmatrix}. \tag{12}$$

The displacement field in the finite rod element can now be represented in terms of the nodal DOFs by eliminating the constant vector $\boldsymbol{a}$ from Eq. 8 by using Eq. 11

$$U(x) = \boldsymbol{N}_R(x,\omega)\boldsymbol{d} \tag{13}$$

where

$$\begin{aligned} \boldsymbol{N}_R(x,\omega) &= \boldsymbol{e}(x,\omega)\boldsymbol{H}_R^{-1}(\omega) = [N_{R1}\ \ N_{R2}], \\ N_{R1}(x,\omega) &= \csc(k_L L)\sin(k_L(L-x)), \\ N_{R2}(x,\omega) &= \csc(k_L L)\sin(k_L x). \end{aligned} \tag{14}$$

The spectral components of the axial force are related to $U(x)$ by

$$N(x) = EAU'(x). \tag{15}$$

The equilibrium condition between the spectral nodal axial forces and the inner forces defined by the strength of the materials yields

$$\boldsymbol{f}_c(\omega) = [N_1\ \ N_2]^T = [-N(0)\ \ +N(L)]^T. \tag{16}$$

Substituting Eq. 13 and Eq. 15 into the right-hand side of Eq. 16 gives

$$\boldsymbol{S}_R(\omega)\boldsymbol{d} = \boldsymbol{f}_c(\omega), \tag{17}$$

in which $\boldsymbol{S}_R(\omega)$ is the spectral element matrix for the finite rod element and is given by

$$\boldsymbol{S}_R(\omega) = \frac{EA}{L}\begin{bmatrix} S_{R11} & S_{R12} \\ S_{R21} & S_{R22} \end{bmatrix} = \boldsymbol{S}_R^T(\omega), \tag{18}$$

where

$$\begin{aligned} S_{R11} = S_{R22} &= \ \ (k_L L)\cot(k_L L), \\ S_{R12} = S_{R21} &= -(k_L L)\csc(k_L L). \end{aligned} \tag{19}$$

2.2 Derivation of the spectral element matrix for a Euler-Bernoulli beam

The partial differential equation of motion for free bending vibration of a Euler-Bernoulli beam is given by

$$EIw'''' + \rho A\ddot{w} = 0, \tag{20}$$

where $w(x,t)$ is the transverse displacement, E is the Young's modulus, A is the cross-sectional area, I is the area moment of inertia and ρ is the mass density. The solution of Eq. 20 is assumed as

$$w(x,t) = \frac{1}{N}\sum_{n=0}^{N-1} W_n(x,\omega_n)\mathrm{e}^{i\omega_n t}. \tag{21}$$

Substituting the approach of Eq. 21 into equation Eq. 20 yields the eigenvalue problem

$$EIW'''' - \omega^2 \rho A W = 0 \tag{22}$$

for each discrete frequency ω_n. The general solution of Eq. 22 is assumed to be

$$W(x) = a\mathrm{e}^{-ik(\omega)x}. \tag{23}$$

Substituting Eq. 23 in Eq. 22 yields the dispersion relation

$$k^4 - k_F^4 = 0 \tag{24}$$

with two real roots and two imaginary roots

$$k_1 = -k_2 = k_F, \quad k_3 = -k_4 = ik_F, \tag{25}$$

where k_F is the wave number of the bending wave mode and is given by

$$k_F = \sqrt{\omega}\left(\frac{\rho A}{EI}\right)^{1/4}. \tag{26}$$

Finally, by inserting the roots in Eq. 23 the general solution for a finite Euler-Bernoulli beam element of length L is given by

$$W(x) = a_1\mathrm{e}^{-ik_F x} + a_2\mathrm{e}^{-k_F x} + a_3\mathrm{e}^{ik_F x} + a_4\mathrm{e}^{k_F x} = \boldsymbol{e}(x,\omega)\boldsymbol{a} \tag{27}$$

with

$$\boldsymbol{e}(x,\omega) = \left[\mathrm{e}^{-ik_F x}\ \mathrm{e}^{-k_F x}\ \mathrm{e}^{+ik_F x}\ \mathrm{e}^{+k_F x}\right], \quad \boldsymbol{a} = [a_1\ a_2\ a_3\ a_4]^T. \tag{28}$$

The values of $\boldsymbol{a}$ depend on the spectral nodal displacements of the finite Euler-Bernoulli beam element, shown in Figure 3, which can be related to the displacement field via

$$\boldsymbol{d} = [W_1\ \theta_1\ W_2\ \theta_2]^T = [W(0)\ \theta(0)\ W(L)\ \theta(L)]^T. \tag{29}$$

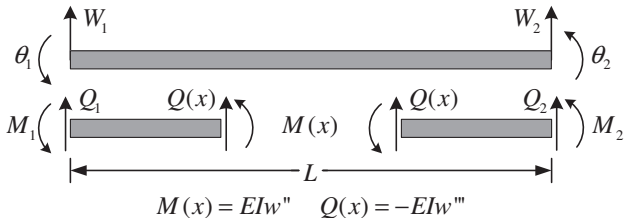

Figure 3. Sign convention for the rod element.

Evaluating Eq. 27 at these nodes yields

$$\boldsymbol{d} = \left[\boldsymbol{e}(0,\omega)\ \boldsymbol{e}'(0,\omega)\ \boldsymbol{e}(L,\omega)\ \boldsymbol{e}'(L,\omega)\right]^T \boldsymbol{a} = \boldsymbol{H}_B(\omega)\boldsymbol{a}, \tag{30}$$

where

$$\boldsymbol{H}_B(\omega) = \begin{bmatrix} 1 & 1 & 1 & 1 \\ -ik_F & -k_F & ik_F & k_F \\ \mathrm{e}^{-ik_F L} & \mathrm{e}^{-k_F L} & \mathrm{e}^{+ik_F L} & \mathrm{e}^{+k_F L} \\ -ik_F\mathrm{e}^{-ik_F L} & -k_F\mathrm{e}^{-k_F L} & ik_F\mathrm{e}^{+ik_F L} & k_F\mathrm{e}^{+k_F L} \end{bmatrix}. \tag{31}$$

By eliminating the constant vector $\boldsymbol{a}$ from Eq. 27 by using Eq. 30, we can represent the displacement field in the finite Euler-Bernoulli beam element in terms of the nodal DOFs with

$$W(x) = \boldsymbol{N}_B(x,\omega)\boldsymbol{d} \tag{32}$$

where

$$
\begin{aligned}
&\boldsymbol{N}_B(x,\omega) = \boldsymbol{e}(x,\omega)\boldsymbol{H}_B^{-1}(\omega) = [N_{B1}\ \ N_{B2}\ \ N_{B3}\ \ N_{B4}],\\
&N_{B1}(x,\omega) = \eta^{-1}k_F\big[\cos\bar{x} - \cos(\bar{L}-\bar{x})\cosh\bar{L} - \cos\bar{L}\cosh(\bar{L}-\bar{x})\\
&\qquad\qquad + \cosh\bar{x} + \sin(\bar{L}-\bar{x})\sinh\bar{L} - \sin\bar{L}\sinh(\bar{L}-\bar{x})\big],\\
&N_{B2}(x,\omega) = \eta^{-1}\big[-\cosh(\bar{L}-\bar{x})\sin\bar{L} + \cosh\bar{L}\sin(\bar{L}-\bar{x}) + \sin\bar{x}\\
&\qquad\qquad - \cos(\bar{L}-\bar{x})\sinh\bar{L} + \cos\bar{L}\sinh(\bar{L}-\bar{x}) + \sinh\bar{x}\big],\\
&N_{B3}(x,\omega) = \eta^{-1}k_F\big[\cos(\bar{L}-\bar{x}) - \cos\bar{x}\cosh\bar{L} - \cos\bar{L}\cosh\bar{x}\\
&\qquad\qquad + \cosh(\bar{L}-\bar{x}) + \sin\bar{x}\sinh\bar{L} - \sin\bar{L}\sinh\bar{x}\big],\\
&N_{B4}(x,\omega) = -\eta^{-1}\big[-\cosh\bar{x}\sin\bar{L} + \cosh\bar{L}\sin\bar{x} + \sin(\bar{L}-\bar{x})\\
&\qquad\qquad + \cos\bar{x}\sinh\bar{L} + \cos\bar{L}\sinh\bar{x} + \sinh(\bar{L}-\bar{x})\big],\\
&\eta = 2k_F(1-\cos\bar{L}\cosh\bar{L}),\\
&\bar{x} = k_F x,\ \ \bar{L} = k_F L.
\end{aligned}
\tag{33}
$$

The spectral components of the bending moment and transverse shear force are related to $W(x)$ by

$$
Q(x) = -EIW'''(x), \quad M(x) = EIW''(x). \tag{34}
$$

The equilibrium condition of the spectral nodal transverse shear forces and bending moments with the corresponding forces and moments defined by the strength of the materials yields

$$
\boldsymbol{f}_c(\omega) = [Q_1\ \ M_1\ \ Q_2\ \ M_2]^T = [-Q(0)\ \ -M(0)\ \ +Q(L)\ \ +M(L)]^T. \tag{35}
$$

Substituting Eq. 32 and Eq. 34 into the right-hand side of Eq. 35 gives

$$
\boldsymbol{S}_B(\omega)\boldsymbol{d} = \boldsymbol{f}_c(\omega), \tag{36}
$$

in which $\boldsymbol{S}_B(\omega)$ is the spectral element matrix for the finite Euler-Bernoulli beam element and is given by

$$
\boldsymbol{S}_B(\omega) = \frac{EI}{L^3}\begin{bmatrix} S_{B11} & S_{B12} & S_{B13} & S_{B14}\\ S_{B12} & S_{B22} & S_{B23} & S_{B24}\\ S_{B13} & S_{B23} & S_{B33} & S_{B34}\\ S_{B14} & S_{B24} & S_{B34} & S_{B44}\end{bmatrix} = \boldsymbol{S}_B^T(\omega), \tag{37}
$$

where

$$
\begin{aligned}
&S_{B11} = S_{B33} = \Delta_B\bar{L}^3(\cos\bar{L}\sinh\bar{L} + \sin\bar{L}\cosh\bar{L}),\\
&S_{B22} = S_{B44} = \Delta_B\bar{L}^3k_F^{-2}(-\cos\bar{L}\sinh\bar{L} + \sin\bar{L}\cosh\bar{L}),\\
&S_{B12} = -S_{B34} = \Delta_B\bar{L}^3k_F^{-1}\sin\bar{L}\sinh\bar{L},\\
&S_{B13} = -\Delta_B\bar{L}^3(\sin\bar{L} + \sinh\bar{L}),\\
&S_{B14} = -S_{B23} = \Delta_B\bar{L}^3k_F^{-1}(-\cos\bar{L} + \cosh\bar{L}),\\
&S_{B24} = \Delta_B\bar{L}^3k_F^{-2}(-\sin\bar{L} + \sinh\bar{L}),\\
&\Delta_B = \frac{1}{1-\cos\bar{L}\cosh\bar{L}},\\
&\bar{L} = k_F L.
\end{aligned}
\tag{38}
$$

The extended spectral element matrix for the Euler-Bernoulli beam element including longitudinal vibrations can be obtained by combining the spectral element matrices for the rod and the Euler-Bernoulli beam, yielding a 6×6 element matrix, which is used for the following calculations.

3 PROBLEM FORMULATION FOR A UNIT-CELL

For an efficient computation using the Spectral Element Method (SEM), an infinitely large structure can be mapped by a representative unit-cell illustrated in Figure 4. The unit-cell of the undeformed lattice is depicted in Figure 4a and the unit-cell of the pre-deformed "zig-zag" lattice is shown in Figure 4b. The periodicity of the structure is accounted for by using the Bloch-Floquet theory. According to the Bloch-Floquet theory, so-called

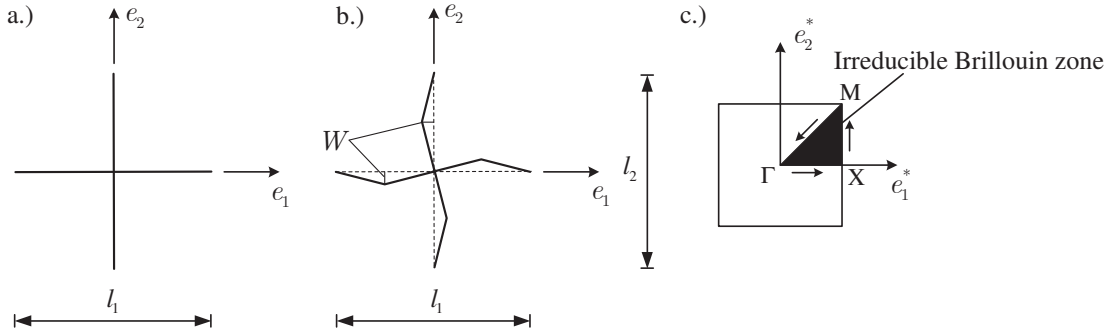

Figure 4. Representative unit-cells of the a.) undeformed and b.) the pre-deformed, "zig-zag" shaped, periodic lattice frame structure. c.) Corresponding irreducible Brillouin zone.

input and output nodes are defined for the unit-cell. A simple 1-D example consisting of 2 spectral elements is illustrated in Figure 5. The first input node is defined on the left side of the unit-cell with the DOFs $D_1,\ D_2,\ D_3$ and the corresponding output node is defined on the right side of the unit-cell with the DOFs $D_7,\ D_8,\ D_9$, respectively. Imposing Bloch-Floquet boundary conditions yields

$$\boldsymbol{D}_{i,out} = [D_7\ D_8\ D_9]^T = \boldsymbol{D}_{i,in}\mathrm{e}^{ik} = [D_1\ D_2\ D_3]^T\mathrm{e}^{ik} \tag{39}$$

and accounts for the periodicity on the right side of the unit-cell. Respectively, the periodicity on the left side of the unit-cell is considered by

$$\boldsymbol{D}_{i,out} = [D_{10}\ D_{11}\ D_{12}]^T = \boldsymbol{D}_{i,in}\mathrm{e}^{-ik} = [D_4\ D_5\ D_6]^T\mathrm{e}^{-ik}, \tag{40}$$

in which $\boldsymbol{k} = [k_x e_1\ k_y e_2]^T$ is the wave vector describing the phase shift of a wave between a unit-cell and it's neighboring unit-cells. The wave vector, in turn, consists of the wave numbers in the $x-$ and $y-$directions, each multiplied by the associated lattice-tiling vectors e_1 and e_2. In the 1-D case considered above the lattice-tiling vector in $y-$direction vanishes and the wave vector is reduced to a scalar.

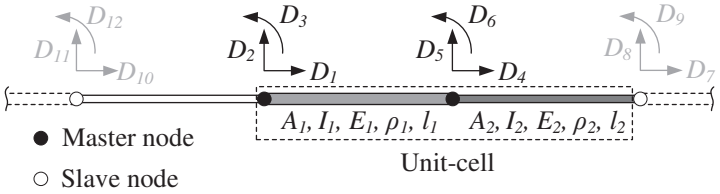

Figure 5. Application of Bloch-Floquet boundary conditions to 1-D unit-cell.

Imposing the boundary conditions reduces the size of the systems spectral matrix from 12×12 to 6×6. Finally, the dispersion curves of the unit-cell, which describe the vibration and wave propagation characteristics of the overall structure, can be determined. For this purpose the eigenvalue problem can be written as

$$\boldsymbol{S}_{ges}(\boldsymbol{\omega},\boldsymbol{k})\boldsymbol{D} = \boldsymbol{0}, \tag{41}$$

which leads to a transcendental equation. This equation has to be solved for for a certain number of wave vectors. The relevant wave vectors are defined by the irreducible Brillouin zone in the reciprocal lattice, as illustrated in Figure 4c. For a more detailed explanation of Bloch-Floquet theory, the Brillouin zone and the determination of dispersion curves the authors refer to (2, 9, 10).

4 EXAMPLE AND DISCUSSION

For the following example, a unit-cell with the sizes $l_1 = l_2 = 100$ mm and the cross-sectional values $A = 15$ mm^2 and $I_y = 10$ mm^4 is analyzed. Furthermore, the material parameters are set to $E = 30000$ MPa and $\rho = 3000$ kg/m^3. The first 8 eigenfrequencies are calculated as functions of the wave vector yielding the corresponding dispersion curves. Without pre-deformation, the calculation results in dispersion curves with no band-gaps in the considered frequency range, as shown in Figure 6a. Accordingly, this means that the vibrations

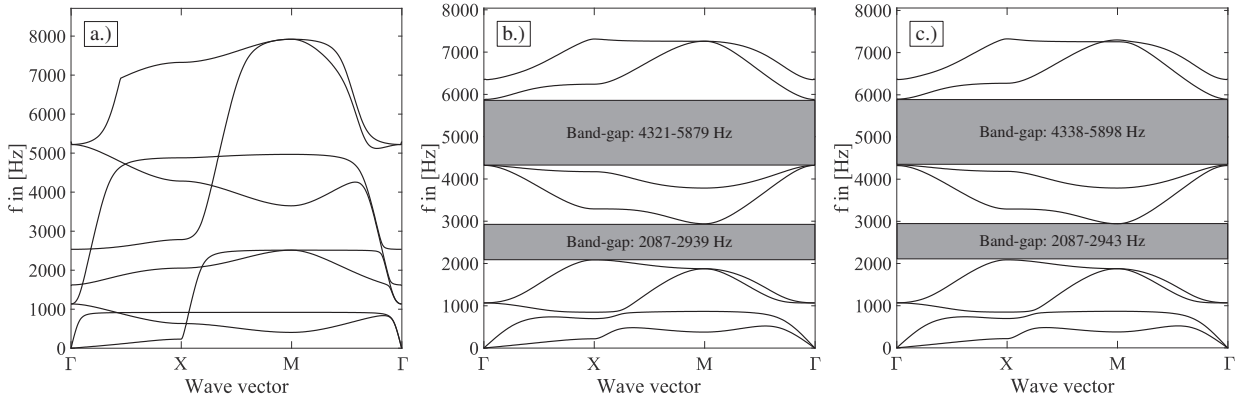

Figure 6. Dispersion curves of the a.) undeformed lattice, b.) the "zig-zag" lattice calculated by SEM ($W = 8$ mm) and c.) the "zig-zag" lattice calculated by FEM with 10 finite elements per beam ($W = 8$ mm).

and elastic waves in the considered frequency range can propagate through the structure. In contrast, in case of a "zig-zag" shaped pre-deformation of the structure with an amplitude $W = 8$ mm, the dispersion curves as shown in Figure 6b exhibit a gap between the 4th and 5th band as well as a gap between the 6th and 7th band. Consequently, the vibrations and elastic waves with a frequency between 2087 and 2939 Hz, respectively between 4321 and 5879 Hz, can not propagate in the structure. Depending on the amplitude and the shape of the pre-deformation, the dispersion curves as presented in Figure 6b can be further optimized, e.g. wider or further band-gaps can be achieved, as shown in (11). The stationary solution for a lattice consisting of 20×20 unit-cells, excited by the frequency $f = 4600$ Hz, is shown in Figure 7. It is obvious, that the propagation of the wave is strongly attenuated.

The dispersion curves for the same unit-cell but calculated with FEM, in which each beam is discretized into 10 finite elements, are shown in 6c.

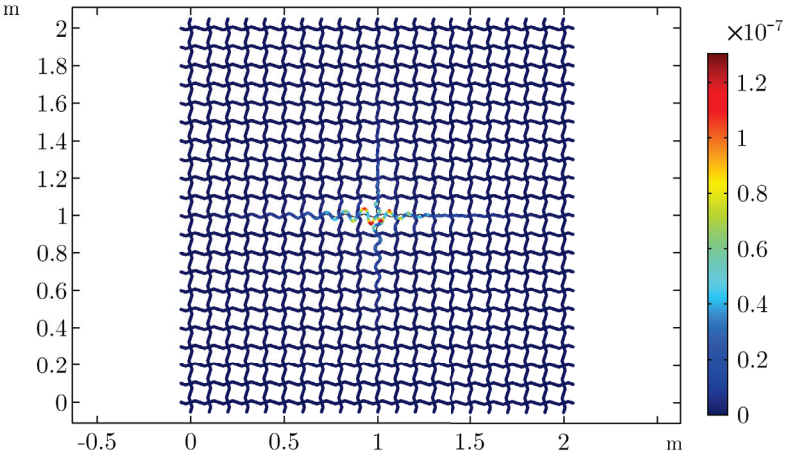

Figure 7. Stationary solution (by COMSOL) of the displacement field for a pre-deformed lattice, with an amplitude of $W = 8$ mm, consisting of 20×20 unit-cells and an excitation of $f = 4600$ Hz at the center.

It is evident, that both methods provide approximately the same results in the considered frequency range. However, while the SEM provides the exact results the FEM only delivers approximate solutions. The accuracy of the FEM strongly depends on the number of nodes per wavelength, this leads to an increased computing time when higher frequency ranges have to be considered.

5 CONCLUSIONS

The properties of a periodic structure can be manipulated by a pre-deformation of the structural elements, in which the band-gaps can be adjusted by both the amplitude and the shape of the pre-deformation. The calculation of the corresponding dispersion curves can be done by the Spectral Element Method, which has the benefit of providing exact results. This is particularly advantageous if higher frequency ranges have to be considered.

REFERENCES

1. Xie, L.; et al. An improved fast plane wave expansion method for topology optimization of phononic crystals. International Journal of Mechanical Sciences, Volume 120, 2016, p. 171-181.
2. Diaz, AR.; Haddow, AG.; Ma, L. Design of band-gap grid structures, Structural and Multidisciplinary Optimization, Vol 29, 2005, p. 418-431.
3. Wang, Y-F.; Wang, Y-S.; Zhang, C. Bandgaps and directional properties of two-dimensional square beam-like zigzag lattices, AIP Advances, Vol 4 (12), 2014, 124403.
4. Yang, C-L.; Zhao, S-D.; Wang, Y-S. Experimental evidence of large complete bandgaps in zig-zag lattice structures, Ultrasonics, Vol 74, 2017, p. 99-105.
5. Khelif, A.; Adibi, A. Phononic Crystals: Fundamentals and Applications, Springer, New York (USA), 1. Edition, 2016.
6. Doyle, JF. Wave Propagation in Structures (Chap. 5), Springer, New York (USA), 1. Edition, 1989.
7. Patera, AT. A spectral element method for fluid dynamics - Laminar flow in a channel expansion, Journal of Computational Physics, Vol 54, 1984, p. 468-488.
8. Lee, U. Spectral Element Method in Structural Dynamics, John Wiley & Sons (Asia) Pte Ltd, Singapore (Republic of Singapore), 1. Edition, 2009.
9. Brillouin, L. Wave Propagation in Periodic Structures, McGraw-Hill Book Company, London (United Kingdom), 1. Edition, 1946.
10. Srikantha Phani, A.; Woodhouse J.; Fleck, NA. Wave propagation in two-dimensional periodic lattices, Acoustical Society of America, Vol 119 (4), 2006, p. 1995-2005.
11. Mellmann, M.; Zhang C. Tuning of vibration and wave propagation characteristics in pre-deformed periodic lattice frame structures, Proceedings in Applied Mathematics & Mechanics 2019, Vol 19, 2019, Accepted but not published yet.